



Poly(*N,N*-bis(2-methoxyethyl)acrylamide), a thermoresponsive non-ionic polymer combining the amide and the ethyleneglycolether motifs

Michelle Hechenbichler¹ · André Laschewsky^{1,2} · Michael Gradzielski³

Received: 29 April 2020 / Revised: 30 June 2020 / Accepted: 1 July 2020 / Published online: 10 August 2020
© The Author(s) 2020

Abstract

Poly(*N,N*-bis(2-methoxyethyl)acrylamide) (PbMOEAm) featuring two classical chemical motifs from non-ionic water-soluble polymers, namely, the amide and ethyleneglycolether moieties, was synthesized by reversible addition fragmentation transfer (RAFT) polymerization. This tertiary polyacrylamide is thermoresponsive exhibiting a lower critical solution temperature (LCST)-type phase transition. A series of homo- and block copolymers with varying molar masses but low dispersities and different end groups were prepared. Their thermoresponsive behavior in aqueous solution was analyzed via turbidimetry and dynamic light scattering (DLS). The cloud points (CP) increased with increasing molar masses, converging to 46 °C for 1 wt% solutions. This rise is attributed to the polymers' hydrophobic end groups incorporated via the RAFT agents. When a surfactant-like strongly hydrophobic end group was attached using a functional RAFT agent, CP was lowered to 42 °C, i.e., closer to human body temperature. Also, the effect of added salts, in particular, the role of the Hofmeister series, on the phase transition of PbMOEAm was investigated, exemplified for the kosmotropic fluoride, intermediate chloride, and chaotropic thiocyanate anions. A pronounced shift of the cloud point of about 10 °C to lower or higher temperatures was observed for 0.2 M fluoride and thiocyanate, respectively. When PbMOEAm was attached to a long hydrophilic block of poly(*N,N*-dimethylacrylamide) (PDMAm), the cloud points of these block copolymers were strongly shifted towards higher temperatures. While no phase transition was observed for PDMAm-b-pbMOEAm with short thermoresponsive blocks, block copolymers with about equally sized PbMOEAm and PDMAm blocks underwent the coil-to-globule transition around 60 °C.

Keywords Polyacrylamide · Water-soluble polymers · Responsive systems · Lower critical solution temperature · Polymer amphiphile

Introduction

Many non-ionic polymers in aqueous solution are thermoresponsive featuring a lower critical solution temperature (LCST), i.e., they are water-soluble or highly

swollen below a characteristic transition temperature but are water-insoluble and collapsed above. Apart from the basic scientific interest in this behavior, its use for a plethora of possible “smart” applications has been discussed [1–3]. While many different polymer chemistries are known to exhibit LCST behavior in aqueous media [4, 5], two major chemical motifs prevail. Water solubility is implemented either via amide moieties or via ethyleneglycol ether groups, as exemplified by the two arguably most studied thermoresponsive polymer systems, namely, poly(*N*-isopropyl acrylamide) (PNIPAm) [6] and polymers based on poly (ethyleneglycol) (PEG) [7, 8]. The specific LCST is mainly determined by the polymer composition, i.e., in the case of homopolymers, by the chemical structure of the underlying monomer. Typically, small chemical changes of the monomer's molecular structure result in big changes of the LCST [4],

✉ André Laschewsky
laschews@uni-potsdam.de

¹ Institut für Chemie, Universität Potsdam, Karl-Liebknecht-Str. 24-25, 14476 Potsdam-Golm, Germany

² Fraunhofer Institut für Angewandte Polymerforschung, Geiselbergstr. 69, 14476 Potsdam-Golm, Germany

³ Stranski-Laboratorium für Physikalische und Theoretische Chemie, Institut für Chemie, Technische Universität Berlin, Straße des 17. Juni 124, Sekr. TC7, 10623 Berlin, Germany

whereat in particular for low-to-moderate molar masses, the precise value can be adjusted to a certain extent by incorporating functional end groups [9–11] or by the precise molar mass itself [4]. A more flexible control over the LCST value is achieved by using statistical copolymers. They can be either obtained by direct copolymerization of appropriate monomers in suitable amounts [12–17] or by partial chemical modification [18–21], and enable the fine-tuning of the LCST value. Yet, except for the rare case of ideal azeotropic copolymerizations (i.e., all copolymerization reactivity ratios are close to unity) [22–27], this gives rise to product mixtures that risk blurring the transition. In any case, the chemical complexity of such thermoresponsive copolymers is increased, which tends to render their chemical analysis as well as the interpretation of experimental findings complicated. This is particularly problematic when additional structural features are to be implemented into thermoresponsive polymers, such as blocky structures or complex functional moieties [28–32]. Therefore, there is a continuous quest for new monomers that yield thermoresponsive homopolymers.

In this general context, we have synthesized and explored polymers of *N,N*-bis(2-methoxyethyl)acrylamide **1** (Fig. 1) with respect to their thermosensitive behavior in aqueous solution. Monomer **1** combines the two dominating chemical motifs of non-ionic thermoresponsive polymers within the same molecule, the amide and ethyleneglycoether moieties, which has been rarely done [33–39]. The monomer does not contain hydrolytically fragile groups such as esters, and its molar mass is rather small compared with the frequently used (oligoethyleneoxide) acrylates and methacrylates [7, 26, 40, 41], which often have the character of macromonomers. Moreover, its chemical structure is close to the ones of the well-established monomers *N,N*-diethylacrylamide (DEAm) and (methoxy diethylene glycol acrylate) (MDEGA), which represent the pure amide and ethyleneglycoether structures. Their polymers exhibit LCSTs in water in the physiologically particularly attractive temperature region of ± 10 °C around human body temperature of 37 °C [23, 42–46]. The thermoresponsivity of the polymers of **1** was mentioned already in the early 1990s [33], but apart from patent claims, polymer **P1** has been hardly studied, and the few data on the aqueous phase behavior are conflicting [36, 47, 48]. Yet, statistical copolymers of *N,N*-dimethylacrylamide and 2-methoxyethylacrylate, which structurally are quite similar to **P1**, have been reported to be both thermosensitive and highly biocompatible [13, 14, 49, 50]. Therefore, we have now explored the use of reversible fragmentation addition chain transfer (RAFT) radical polymerization, to prepare homopolymers of **1** of targeted molar masses. We also synthesized diblock copolymers of **1** with the strongly hydrophilic comonomer *N,N*-dimethylacrylamide **2** (Fig. 1) and investigated the

thermoresponsive behavior of the various polymers in dilute aqueous solution.

Experimental

Materials

Acetone-d₆ (≥ 99.5 atom% D, Armar Chemicals (Europa), Leipzig, Germany), acryloyl chloride ($\geq 96.0\%$, stabilized with phenothiazine, Merck), allyltrimethylsilane (98%, abcr, Karlsruhe, Germany), aluminum oxide (Al₂O₃ activated basic, Brockmann I, Sigma–Aldrich), benzene (99.5%, Carl Roth GmbH, Karlsruhe, Germany), benzyl bromide (99%, Alfa Aesar), *N,N*-bis(2-methoxyethyl) amine ($> 98.0\%$, TCI Deutschland GmbH, Eschborn, Germany) carbon disulfide ($\geq 99.9\%$, Merck), chloroform ($\geq 99.5\%$, stabilized with amylene, Th. Geyer, Renningen, Germany), chloroform-d (99.8 atom% D, Armar Chemicals), 4-chloromethylbenzoyl chloride ($> 98\%$, TCI), deuterium oxide (99.8 atom% D, Armar Chemicals), dichloromethane ($\geq 99.8\%$, stabilized with amylene, Th. Geyer), diethylether ($\geq 99.5\%$, Th. Geyer), *n*-dodecyl-1-amine (97%, Alfa Aesar, ethanol, (abs, Merck)), ethyl acetate (99.9%, VWR International GmbH, Darmstadt, Germany), *n*-hexane, (99.0%, Th. Geyer), aqueous hydrochloric acid (HCl, 1 M, Th. Geyer), magnesium sulfate (anhydrous $\geq 99.5\%$, Alfa Aesar), methanol (technical grade, Merck), methanol (for spectroscopy, Uvasol grade, Merck), petrol ether (b.p. 60–80 °C, analytical grade, Th. Geyer), propane-1-thiol (98%, Alfa Aesar), pyridine (anhydrous $> 99.0\%$, Alfa Aesar), pyrrolidine (99%, Merck), sodium hydroxide ($\geq 98.8\%$, Th. Geyer), tetrahydrofuran ($\geq 99.9\%$, stabilized with 2,6-di-*t*-butylbutyl-*p*-cresol “BHT”, Th. Geyer), thioacetic acid ($\geq 98\%$, Merck), and triethylamine (99%, Acros Organics/Fisher Scientific GmbH, Schwerte, Germany) were used as received. 1,1'-Azobis (cyclohexanecarbonitrile) V-40 (98%, Sigma–Aldrich) and 2,2'-Azobis(2-methylpropionitrile) AIBN (98%, Sigma–Aldrich) were crystallized from chloroform (V-40) or *n*-hexane (AIBN) prior to use. *N,N*-dimethylacrylamide (DMAm **2**, $\geq 99.0\%$, stabilized with 4-methoxyphenol “MEHQ”) was distilled prior to use. Deionized water was used for synthesis. For measurements, deionized water was further purified by a Millipore Milli-Q Plus water purification system (Merck Millipore, Darmstadt, Germany), resistivity 18 m Ω cm⁻¹. Column chromatography was performed on Silica Gel 60 (0.063–0.200 mm, 230–400 mesh ASTM, Merck).

Chain transfer agent (CTA) benzylpropylcarbonotrithioate (BPTC, **3**) was prepared from 1-propanethiol, CS₂, and benzylbromide, adapting reported procedures [51, 52]. The raw product was purified by column chromatography on silica gel using the mixture petroleum ether:ethyl acetate 40:1 (v/v). The analytical data agreed with the reported ones [52, 53].

Synthesis of *N,N*-bis(2-methoxyethyl)acrylamide (bMOEAm, 1)

A solution of acryloyl chloride (11.3 mL, 12.6 g, 0.139 mol, 1.1 eq.) in CH_2Cl_2 (40 mL) was dropped over 3 h into a stirred solution of bis(2-methoxyethyl) amine (18.7 mL, 16.8 g, 0.127 mol) and triethylamine (26.5 mL, 19.3 g, 0.191 mol, 1.51 eq.) in CH_2Cl_2 (350 mL) at 0 °C. The reaction mixture was allowed to warm up to ambient temperature and continued to be stirred overnight. The precipitated triethylammonium hydrochloride was filtered off and washed with CH_2Cl_2 (100 mL). The combined organic solutions were extracted subsequently with 1 M HCl (3 × 50 mL), water (50 mL), and brine (100 mL). The organic layer was dried over anhydrous MgSO_4 and the solvent removed under reduced pressure. The raw product was purified by vacuum distillation to give a viscous liquid ($n_{20}^D = 1.4722$). Yield: 14.5 g (61%)

$^1\text{H-NMR}$ (300 MHz in CDCl_3 , δ in ppm): $\delta = 3.11$ (s, 6H, CH_3), 3.27–3.43 (m, 6H, N- CH_2 - CH_2 -O), 5.44 (dd, 1H, $\text{CH}^E = \text{C-CO}$), 6.09 (dd, 1H, $\text{CH}^Z = \text{C-CO}$), 6.46 (dd, 1H, = CH-C=O)

$^{13}\text{C-NMR}$ (75 MHz in CDCl_3 , δ in ppm): $\delta = 46.45$ (N- CH_2), 48.33 (N- CH_2), 58.16 (O- CH_3), 58.43 (O- CH_3), 70.53 (CH_2 -O), 126.93 (CH_2 -CH), 127.71 (CH-CO), 166.11 (CO)

Elemental analysis, calculated: $\text{C}_9\text{H}_{17}\text{NO}_3$: C 57.7%, H 9.2%, N 7.5%, found: C 56.7%, H 10.9%, N 7.4%

Mass spectrometry: calculated mass M_r : 188.1287 g/mol, found mass: 188.1291 g/mol

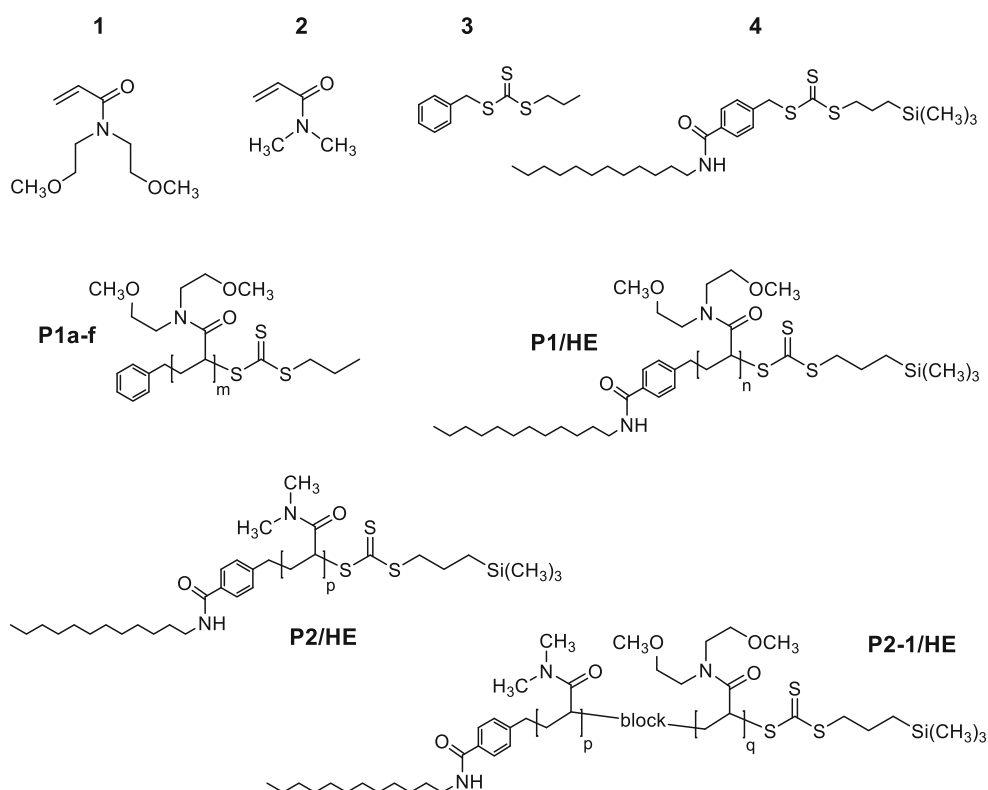
FTIR (selected bands cm^{-1}): 2982, 2929, 2883, 2821, 1647, 1610, 1443, 1363, 1189, 1111, 1012, 978, 960, 795

Synthesis of 4-chloromethyl-*N-n*-dodecylbenzamide

4-Chloromethylbenzoyl chloride (25.5 g, 0.135 mol) was dissolved in CHCl_3 (20 mL) and cooled down to 0 °C. Pyridine (21.5 mL, 21.0 g, 0.266 mol, 1.97 eq.) was added. Subsequently, dodecylamine (25.1 g, 0.136 mol, 1.1 eq.) was added slowly. The mixture was stirred at room temperature overnight. Then, CHCl_3 (150 mL) was added, the mixture was extracted with 1 M aqueous HCl (100 mL), and the aqueous phase was re-extracted with CHCl_3 (3 × 50 mL). The combined organic phases were washed with 1 M HCl (100 mL) and distilled water (100 mL). The resulting emulsion was split by adding NaOH (23.3 g). The combined organic phases were washed with brine (500 mL). After drying over MgSO_4 , the solvent was removed under reduced pressure. The residue was crystallized twice from MeOH and twice from ethyl acetate and dried in vacuo to yield a colorless solid (16.05 g, 35%).

$^1\text{H-NMR}$ (300 MHz in CDCl_3 , δ in ppm): $\delta = 0.88$ (t, 3H, CH_3), 1.26–1.33 (m, 18H, -(CH_2)₉), 1.61 (m, 2H, N- C-CH_2), 3.44 (dt, 2H, N- CH_2), 4.60 (s, 2H, C- CH_2 -S), 6.14 (broad t, 1H, N-H), 7.44 (d, 2H, $\text{ArH}^{2,6}$), 7.75 (d, 2H, $\text{ArH}^{3,5}$)

Fig. 1 Structure of the monomers, chain transfer agents (CTA), and polymers synthesized



Synthesis of 3-(trimethylsilyl)propane-1-thiol

Adapting a literature procedure [54], allyltrimethylsilane (33.5 mL, 24.1 g, 211 mmol) was dissolved in THF (120 mL). Thioacetic acid (29.0 mL, 26.9 g, 353 mmol, 1.67 eq.) and AIBN (0.273 g, 1.66 mmol, 0.01 eq.) were added and the solution was refluxed under inert gas for 23 h. After cooling, 10 wt% aqueous NaOH (100 mL) was added at 0 °C while stirring. The organic solvent was removed under reduced pressure and the residue was dissolved in ethyl acetate (100 mL). The organic phase was washed with 10 wt% NaOH (3 × 100 mL, 3 × 50 mL) and distilled water (100 mL). The combined aqueous phases were extracted with ethyl acetate (100 mL). The combined organic phases were washed with distilled water (100 mL) and brine (100 mL) and dried over MgSO₄. Afterwards, the solvent was removed under reduced pressure to give S-(4-(trimethylsilyl)propyl) ethanethioate as colorless liquid (38.7 g, 0.203 mol, 94%).

¹H-NMR (300 MHz in CDCl₃, δ in ppm): δ = -0.02 (s, 9H, Si-CH₃), 0.56 (m_c, 2H, Si-CH₂), 1.61–1.50 (m, 2H, CH₂-CH₂), 2.32 (s, 3H, CO-CH₃), 2.87 (t, 2H, CH₂-S)

The so obtained intermediate thioester (41.3 g, 0.217 mol) was dissolved in ethanol and cooled to 0 °C. A 25 wt% NaOH solution (1.5 eq.) was added and the reaction mixture was stirred overnight. Thin layer chromatography (TLC) showed completely consumption of the educt. The reaction mixture was neutralized with conc. HCl, and extracted twice with CH₂Cl₂ (100 mL, 40 mL). The combined organic phases were washed with distilled water (3 × 100 mL), 10 wt% NaOH (3 × 50 mL), distilled water (100 mL), and brine (100 mL). After drying over MgSO₄, the solvent was removed under reduced pressure. The residue was distilled in vacuo to give 3-(trimethylsilyl)propane-1-thiol as colorless liquid (12.4 g, 83.7 mmol, 66%).

¹H-NMR (300 MHz in CDCl₃, δ in ppm): δ = -0.01 (s, 9H, Si-CH₃), 0.58 (m_c, 2H, Si-CH₂), 1.34 (t, 1H, S-H), -, 1.65–1.55 (m, 2H, CH₂-CH₂), 2.52 (dt, 2H, CH₂-S)

Synthesis of 4-(dodecylcarbamoyl)benzyl-3-(trimethylsilyl)propyl carbonotrithioate (4dBtmsPTC, 4)

S-(4-(Trimethylsilyl)propyl) ethanethiol (8.22 g, 55.4 mol) and CS₂ (3.35 ml, 4.22 g, 55.4 mmol, 1.00 eq.) were dissolved in dry CH₂Cl₂ (20 mL) and stirred at room temperature. Triethylamine (7.90 mL, 5.77 g, 57.1 mmol, 1.03 eq.) was added dropwise, while keeping the reaction at room temperature. The orange solution formed was stirred for 30 min. 4-Chloromethyl-*N*-dodecylbenzamide (17.79 g, 52.64 mmol, 0.95 eq.) was slowly added, and the reaction was stirred overnight. After dilution with more CH₂Cl₂ (40 mL), the solution was washed with water (3 × 100 mL), the collected aqueous phases re-extracted with CH₂Cl₂ (20 mL), and the combined

organic phases finally washed with brine and dried over MgSO₄. The organic solvent was removed under reduced pressure, and the raw product purified by two subsequent column chromatographies on silica gel using petrol ether:ethyl acetate (first with gradient: 10:1 (v/v) increasing to 10:4 (v/v); second with a fixed ratio of 20:1 (v/v)). Yield: 9.67 g, 18.4 mmol (39%), yellow wax

¹H-NMR (300 MHz in CDCl₃, δ in ppm): δ = -0.01 (s, 9H, Si-(CH₃)₃), 0.61 (m_c, 2H, Si-CH₂), 0.88 (t, 3H, CH₃), 1.25–1.32 (m, 18H, CH₃-(CH₂)₉), 1.57–1.70 (m, 4H, N-CH₂-CH₂ & S-CH₂-CH₂), 3.35–3.46 (m, 4H, N-CH₂ & S-CH₂-CH₂), 4.63 (s, 2H, C-H₂-S), 6.12 (br. t, 1H, N-H), 7.39 (d, 2H, ArH^{2,6}), 7.70 (d, 2H, ArH^{3,5})

¹³C-NMR (75 MHz in CDCl₃, δ in ppm): δ = -1.63 (Si-CH₃), 14.21 (CH₃-CH₂), 16.69 (Si-CH₂), 22.81 (CH₃-CH₂), 23.15 (Si-CH₂-CH₂), 27.15 (N-(CH₂)₂-CH₂), 29.47–29.84 (N-(CH₂)₂-CH₂-(CH₂)₆), 32.05 (CH₃-CH₂-CH₂), 40.29 (S-CH₂-CH₂), 40.68 (N-CH₂), 40.81 (Ar-CH₂), 127.33 (ArC^{3,5}), 129.51 (ArC^{2,6}), 134.44 (ArC⁴), 139.09 (ArC¹), 167.10 (CO), 223.39 (CS)

Elemental analysis, calculated: C₂₇H₄₇NOS₃Si: C 61.7%, H 9.0%, N 2.7%, S 18.3% found: C 61.5%, H 9.0%, N 2.6%, S 17.6

Electron ionization mass spectrometry: C₂₇H₄₈NOS₃Si: calculated mass M_r: 526.2662 g/mol, found: m/z: 526.2663 g/mol

FTIR (selected bands cm⁻¹): 2953, 2920, 2850, 1632, 1533, 1504, 1468, 410, 1300, 1248, 1061, 949, 860, 831, 808, 719, 688

Homopolymerization of *N,N*-bis(2-methoxyethyl) acrylamide (P1)

In a typical procedure, monomer **1** (1.00 g, 5.34 mmol, 25 eq.) and CTA **3** (51.19 mg, 0.2112 mmol) were dissolved in benzene (2.00 mL) at ambient temperature. 2.57 mL of a stock solution of V-40 in benzene (2.00 mg mL⁻¹) equivalent to 0.0212 mmol of initiator was added, and the homogenous reaction mixture were purged with N₂ for 45 min. The mixture was immersed into an oil bath preheated to 90 °C and stirred. After 5 h, the polymerization was quenched by opening the flask to the air and cooling the mixture with an isopropanol/dry ice bath. After warming to room temperature, 5 mL of THF were added, and the polymer was isolated by precipitation into diethylether. After drying in the vacuum oven (40 °C, 1 mbar), the polymer was dissolved in water and lyophilized to obtain a viscous, yellowish mass. Yield: 0.82 g (78%)

Various homopolymer samples were prepared by varying the relative amounts of monomer **1**, CTA, and initiator V-40 (series **P1**), or by substituting CTA **3** by CTA **4** (series **P1/HE**), while maintaining throughout a 10:1 M ratio of CTA:initiator.

Homopolymerization of *N,N*-dimethylacrylamide (P2/HE)

Monomer **2** (17.5 mL, 16.9 g, 0.170 mol, 202 eq.), CTA **4** (442.6 mg, 0.8415 mmol, 1 eq.), and V-40 (20.6 mg, 0.0843 mmol, 0.1 eq.) in benzene (76 mL) were purged with N₂ for 45 min. The mixture was placed into a preheated oil bath at 90 °C and stirred for 3 h. Then, the polymerization was quenched by opening the flask to the air and rapid cooling. The polymer was isolated and purified by precipitating twice into diethylether. The collected polymer **P2/HE** was dried in the vacuum oven, dissolved in water, and lyophilized. Yield: 10.98 g (63%) hygroscopic yellow powder

Synthesis of block copolymers P2-1/HE

In a typical procedure, monomer **1** (1.02 g, 5.44 mmol, 100 eq.) and macroCTA **P2/HE** (0.87 g, 0.054 mmol) were dissolved in benzene (17.0 mL) at ambient temperature. 0.67 mL of a stock solution of V-40 in benzene (2 mg mL⁻¹) equivalent to 0.0055 mmol were added. The solution was purged with N₂ for 45 min and placed into a preheated oil bath with a temperature of 90 °C. After stirring for 3 h, the reaction was stopped by opening the flask to the air and cooling the flask with liquid nitrogen. The polymer **P2-1b/HE** was isolated and purified by twice repeated precipitations into diethylether. The polymer was dried in the vacuum oven, dissolved in water, and lyophilized. Yield: 1.34 g (71%), hygroscopic yellow powder

Methods and instrumentation

Elemental analysis was performed with a Vario ELIII micro-analyzer (Elementar Analysensysteme, Hanau, Germany). Refractive indexes were determined with a NAR-3T refractometer (ATAGO CO., LTD., Tokyo, Japan) equipped with a DTM-3 thermostat. NMR spectra were recorded using a Bruker Avance 300 NMR spectrometer operating at 300 MHz for ¹H measurements and 75 MHz for ¹³C measurements. Chemical shifts δ are given in ppm referring to the respective solvent peaks at δ (¹H) 7.26 ppm and δ (¹³C) 77.16 ppm for CDCl₃, and at δ (¹H) 4.79 ppm for D₂O. Fourier-transform infrared spectroscopy (FTIR) spectra were recorded using a Nicolet Avatar 370 FTIR spectrometer (Thermo Fisher Scientific) equipped with an ATR Smart Performer element and AMTIR crystal.

Polymers were analyzed by size exclusion chromatography (SEC) in NMP + 0.1% LiBr with simultaneous UV and RI detection at room temperature (flow rate 0.5 mL min⁻¹). The stationary phase used was a 300 × 8 mm² PSS GRAM linear M column (7 μ m particle size). Samples were filtered through 0.45- μ m filters and the injected volume was 100 μ L.

Narrowly distributed polystyrene standards (PSS, Mainz, Germany) were used for calibration.

UV/Vis spectra were recorded on a PerkinElmer Lambda 25 UVVis Spectrometer, using quartz sample cells with 1 cm path length. Number average molar masses M_n^{UV} were calculated by end group analysis, using the extinction E at 309 nm of the π - π^* transition of the trithiocarbonate chromophore in methanol. Values were calculated according to $M_n^{UV} = \epsilon \cdot c \cdot d \cdot E^{-1}$ where ϵ (L mol⁻¹ cm⁻¹) is the extinction coefficient, c (g L⁻¹) is the concentration of the polymer in solution, and d (cm) is the optical path length. The molar extinction coefficient ϵ of the trithiocarbonate chromophore was assumed to be 15,800 L mol⁻¹ cm⁻¹ at 309 nm in methanol, due to the structural similarity of the polymer bound trithiocarbonate end groups with the references 2-(((butylthio)carbonothioyl)thio) propanoic acid and *N,N*-dimethyl-2-(((butylthio)carbonothioyl)thio) propionamide [55].

Thermogravimetric analysis (TGA) was conducted under N₂ purged atmosphere using an apparatus SDTA851e (Mettler-Toledo, Giessen, Germany), in the temperature range from 25 to 900 °C with a heating rate of 10 K min⁻¹. Differential scanning calorimetry (DSC) was performed with an apparatus DSC822e (Mettler-Toledo, Giessen, Germany), applying heating and cooling rates of 10 K min⁻¹ for the first and second, and 30 K min⁻¹ for the third and fourth heating and cooling cycles. Glass transition temperatures T_g were taken from the second heating cycle that used a heating rate of 10 K min⁻¹ via the midpoint method [56].

Dynamic light scattering (DLS) was carried out with a high-performance particle sizer (HPPS-5001, Malvern Instrument, Malvern, UK) using a He-Ne laser beam and a thermoelectric Peltier element to control the temperature of the sample cell. The backscattering mode was used at a scattering angle of $\Theta = 173^\circ$. Samples were prepared by dilution with Millipore water to the desired concentration, and measured in heating runs by raising the temperature in steps of 1 °C equilibrating the sample for 120 s prior to each measurement. Temperature-dependent turbidimetry measurements were performed with a Cary 5000 (Varian) spectrometer with heating and cooling rates of 0.5 K min⁻¹. Temperatures are precise within 0.5 K.

Results and discussion

Monomer *N,N*-bis(2-methoxyethyl)acrylamide **1** was synthesized by the straightforward reaction of the amine with acryloylchloride, adapting previous procedures [33, 47], and the so far scarce molecular analytical data available were completed. Figure 2 displays the ¹H and ¹³C NMR spectra in CDCl₃. The duplication of methylene signal characteristic for the 2-methoxyethyl substituents on the amide nitrogen

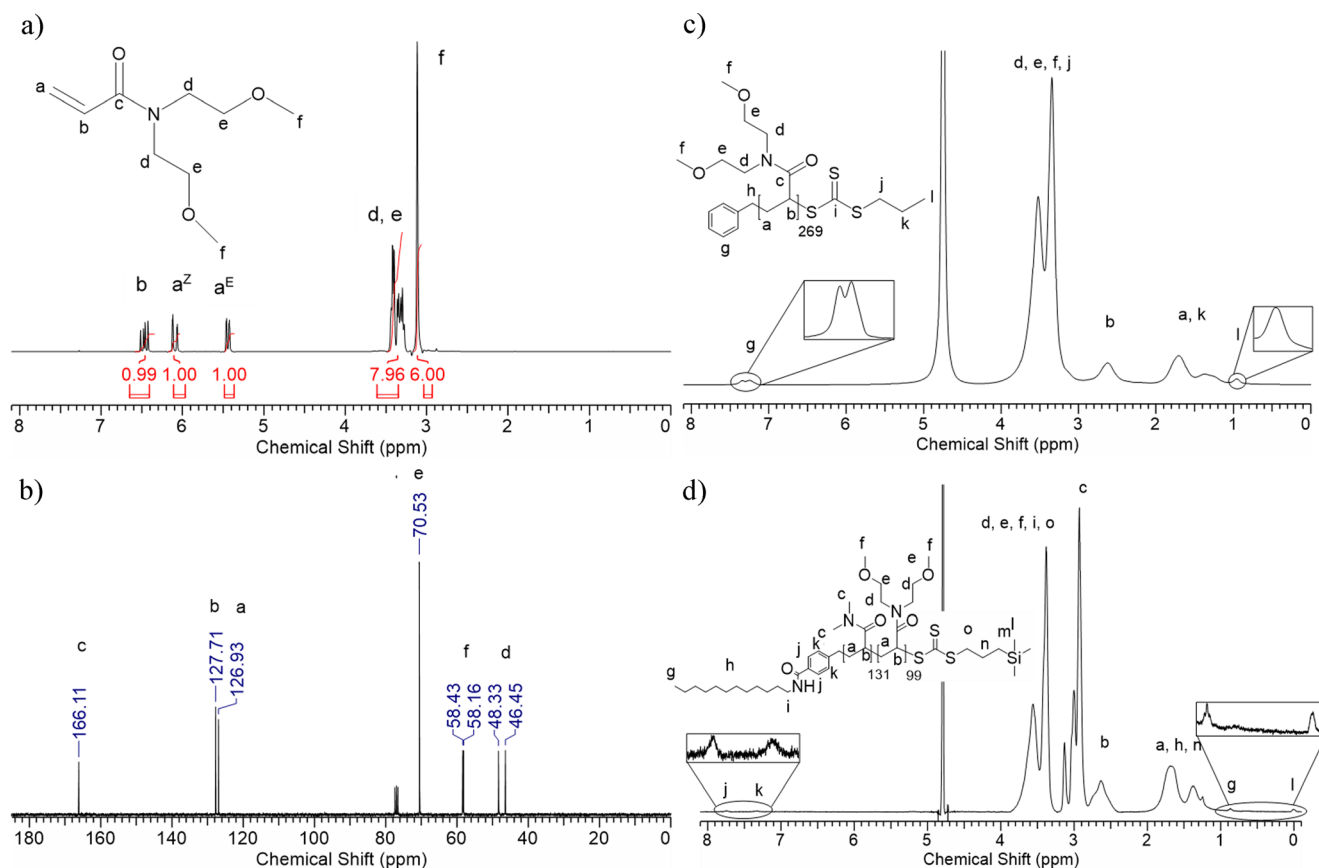


Fig. 2 (a) ^1H -NMR spectrum and (b) ^{13}C -NMR spectrum of monomer bMOEAm **1** in CDCl_3 ; ^1H -NMR spectra of (c) homopolymer **P1e** and (d) block copolymer **P2-1b/HE** in D_2O

between 3.4 and 3.7 ppm is caused by the ambient temperature still relatively slow exchange (compared with the NMR frequency) between the trans- and cis-positions of the amide substituents, so that the respective signal groups do not completely coalesce.

Initially, monomer **1** was homopolymerized by radical polymerization employing the RAFT method to control molar masses and minimize the polymers' dispersities, \bar{D} . For preparing a series of increasing molar masses of **P1**, the established RAFT agent S-benzyl-S'-propyl trithiocarbonate **3** was employed as CTA [52, 53]. The polymerization recipes are compiled in Table 1, and the key characteristics of the obtained polymers in Table 2. The resulting general structure is displayed in Fig. 1, and a typical ^1H NMR spectrum in Fig. 2(c). In analogy to statistical copolymers of 2-methoxyethylacrylate and *N,N*-dimethylacrylamide **2** [14], all polymers **P1** were soluble in a large variety of solvents of strongly differing polarities, such as cold water, methanol, ethanol, trifluoroethanol, hexafluoroisopropanol, acetonitrile, *N*-methylpyrrolidone (NMP), dimethylsulfoxide (DMSO), ethyl acetate, acetone, α,α,α -trifluorotoluene, dioxane, tetrahydrofuran (THF), chloroform, dichloromethane, and benzene. Only diethylether and plain hydrocarbons such as pentane and hexane were found to be nonsolvents.

Due to the low molar mass of the sample **P1b** shown (Fig. 2(c)), characteristic signals of both end groups can be easily distinguished in the spectrum, namely, of the phenyl moiety originating from the R-group of CTA **3** at 7.1 to 7.3 ppm, and of the methyl moiety of the *n*-propyl residue originating from the Z-group at about 0.9 ppm. These signals enable the calculation of the number average molar mass M_n using either of the two end groups (denoted $M_n^{\text{NMR-R}}$ and $M_n^{\text{NMR-Z}}$). However, the accuracy inevitably decreases rapidly with increasing molar masses. Additionally, the thiocarbonyl moiety of the Z-group is a strong UV-chromophore with an absorbance maximum in the range of 305–310 nm and an extinction coefficient ε in the order of $10^4 \text{ L mol}^{-1} \text{ cm}^{-1}$. This allows for a rather sensitive determination of the polymer's Z-group content even for high molar masses when the value of ε is known, and, thus, also to derive a number average molar mass value, denoted M_n^{UV} [55]. Moreover, assuming ideal conditions for the RAFT polymerization process, the theoretically expected number average molar mass M_n^{theo} can be calculated from the molar ratio of the monomer to the RAFT agent employed that is corrected by the monomer conversion. Furthermore, size exclusion chromatography (SEC) was used to analyze the molar mass distribution, and to calculate therefrom apparent number average molar masses M_n^{app} (calibrated to polystyrene)

Table 1 Reaction conditions for polymerization in benzene using initiator V-40

Sample	Monomer	Amount (mmol)	CTA	Amount (mmol)	Initiator (mmol)	Yield (%)
P1a	1	5.36	3	0.569	0.057	68
P1b	1	5.34	3	0.211	0.021	78
P1c	1	5.52	3	0.104	0.010	68
P1d	1	5.23	3	0.033	0.003	61
P1e	1	5.33	3	0.020	0.002	91
P1f	1	5.39	3	0.010	0.001	91
P1/HE	1	14.4	4	0.095	0.007	59
P2/HE	2	170	4	0.842	0.084	63
P2-1a/HE	1	6.41	P2/HE	0.159	0.016	79
P2-1b/HE	1	5.44	P2/HE	0.054	0.005	71

and the dispersities \bar{D} . Altogether, the comparison of the various analytical molar mass data allows judging the controlled character of the polymerization, and, in particular, to estimate the degree of Z-group fidelity, i.e., the percentage of the polymer chains that bear an active end group. This is a crucial information for successful further chain extension as in the synthesis of block copolymers.

Analyzing the data for **P1a–P1f**, we note in general relatively low dispersities \bar{D} of 1.2–1.3, and good agreement of M_n^{theo} and $M_n^{\text{NMR-R}}$. This suggests that the RAFT polymerization of **1** is well controlled. We note that the M_n^{app} values derived from SEC systematically underestimate the molar masses of the **P1** samples, i.e., the calibration using polystyrene standards is not optimal. Furthermore, we find that the $M_n^{\text{NMR-Z}}$ and M_n^{UV} values agree reasonably well with the values of M_n^{theo} and $M_n^{\text{NMR-R}}$, indicating good preservation of the RAFT-active trithiocarbonate end group. Still, it

appears that the $M_n^{\text{NMR-Z}}$ and in particular the M_n^{UV} values tend to become higher than the $M_n^{\text{NMR-R}}$ values with increasing molar masses, pointing to an increasing loss of active end groups. To a certain extent, such a loss is inevitable due to the inherent RAFT mechanism [57]. Moreover, the ether functions of **1** that are prone to radical side reactions via hydrogen abstraction might contribute to the loss. In any case, if molar masses up to 20,000 are aspired, the data demonstrate that RAFT polymerization of **1** proceeds smoothly. Even for higher molar masses, the extent of polymerization control is still reasonably good.

Additionally, we undertook preliminary experiments exploring the use of functionalized RAFT agent **4** for the polymerization of **1**, in the perspective of synthesizing thermoresponsive polymeric surfactants. The mixed aliphatic-aromatic *N*-dodecylbenzamide moiety of the R-group of **4** will confer the needed segmental hydrophobic

Table 2 Molecular characteristics of the polymers synthesized

Sample	M_n^{theo} (kg mol^{-1})	DP_n^{theo}	$M_n^{\text{NMR-R}}$ (kg mol^{-1})	$DP_n^{\text{NMR-R}}$	$M_n^{\text{NMR-Z}}$ (kg mol^{-1})	M_n^{UV} (kg mol^{-1})	M_n^{app} (kg mol^{-1}) ^a	\bar{D} ^a	T_g (°C)
P1a	1.9	9	2.1	10	2.1	2.1	1.4	1.20	−9
P1b	4.9	25	5.5	28	5.7	4.9	3.2	1.22	−2
P1c	10.2	53	10.4	54	9.8	15	6.3	1.26	6
P1d	31.7	168	31	163	27	44	18	1.21	8
P1e	50.6	269	57	303	59	180	27	1.39	10
P1f	99.1	528	− ^b	− ^b	98	93	51	1.23	9
P1/HE	29.0	152	30	157	35	37	12.6	1.46	n.a.
P2/HE	13.5	131	16	155	16	14	14	1.18	119
P2-1a/HE	20.8	131 + 39 ^c	25	131 + 47 ^c	59	78	18	1.16	80
P2-1b/HE	39.1	131 + 99 ^c	30	131 + 90 ^c	− ^b	− ^b	26	1.17	58

n.a. not available

^a By SEC, eluent NMP, calibration with polystyrene standards

^b No end group signal detected

^c First number refers to **P2** block, second number to **P1** block

character to polymers of structure **P1/HE** (see Fig. 1). Importantly, the use of CTA **4** albeit somewhat cumbersome to synthesize attaches the hydrophobic end groups by hydrolytically inert C-C bonds to such polymeric surfactants. This is an important advantage over most reported hydrophobized RAFT agents, where the hydrophobe is placed in the so-called Z-group that is inherently sensitive to hydrolysis [58–64]. Moreover, the particular choice of the various building blocks of CTA **4** was aimed at supporting polymer end group analysis by ^1H NMR, as they simplify the identification and quantification of both the R- and Z-groups attached to the polymers in the spectra [65–67]. For instance, the signals of the aryl protons in ortho position to the carboxyl moiety of the R-group appear close to 8 ppm, while the signal of the trimethylsilyl groups of the Z-group is positioned close to 0 ppm, i.e., in regions that are devoid of signals for most polymers and solvents used in NMR analysis. This allows not only the determination of the true number average molar masses M_n but enables also the first-hand estimation of the RAFT-active end group fidelity by comparing the integrated signals specific to the R- and Z-groups. Both informations are generally difficult to obtain, especially in the case of amphiphilic polymers which, e.g., often tend to interact either with SEC column material, and/or to associate in the eluent.

In a second stage, we explored the use of monomer **1** for constructing thermoresponsive block copolymers. For this purpose, we first polymerized monomer **2**, *N,N*-dimethylacrylamide (DMAm), to produce a polymer that is water-soluble over the full temperature range between 0 and 100 °C [23, 68], using the RAFT agent **4**. Subsequently, we employed this homopolymer **P2/HE** as macroCTA for the chain extension with monomer **1**. This yields block copolymers with a permanently hydrophobic end group at one terminus of the polymer chain (due to the use of CTA **4**), and a hydrophilic-to-hydrophobic reversibly “switchable” end block made of the polymer of **1** on the opposite terminus (see Fig. 1). This design results in a polymer surfactant architecture which can be thermally switched between the structure of classical polymeric surfactants with one hydrophobic end group (similar to fatty alcohol ethoxylates) and the one of associative telechelics that dispose of two, here nonsymmetrical, hydrophobic end groups [69]. Key molecular data of the various polymers prepared with CTA **4** are listed in Table 2. For homopolymers **P1/HE** and **P2/HE**, we note good agreement not only between the M_n^{theo} and $M_n^{\text{NMR-R}}$ values, but also with the respective values $M_n^{\text{NMR-Z}}$. This finding, together with the low dispersities \bar{D} of 1.2 for **P2/HE**, suggests that the RAFT polymerization using CTA **4** is also well controlled. Still, notwithstanding the good agreement of the values for M_n^{theo} , $M_n^{\text{NMR-R}}$ and $M_n^{\text{NMR-Z}}$, sample **P1/HE** presents a relatively high dispersity of 1.4–1.5 in the SEC analysis. Also, the M_n^{app} value even more underestimates the true molar mass of **P1/HE** than we noted for the series of samples

P1a–P1f prepared using CTA **3**. These apparently inconsistent findings might be due to some weak interaction of the end-functionalized polymer **P1/HE** with the column material, thus provoking a tailing of the elugram towards longer elution times, which consequently reduces M_n^{app} but increases \bar{D} . In any case, the analytical data show that the trithiocarbonate group is largely preserved, and sample **P2/HE** represented a good macroCTA for the chain extension with monomer **1**. The data in Tables 1 and 2 also demonstrate the successful chain extension up to high conversions to produce the block copolymers **P2-1a/HE** and **P2-1b/HE**. Still, the analytical data indicate that the RAFT-active trithiocarbonate group was largely lost at the end of the chain extension step, despite the low values of about 1.2 for \bar{D} .

Thermal analysis showed that the polymers were thermally stable up to at least 200 °C according to thermogravimetric analysis TGA (Fig. 3(a)), when presumably the decomposition of the trithiocarbonate end groups sets in [70, 71]. Notable mass loss took only place at temperatures beyond 300 °C. Differential scanning calorimetry showed (compared with most reported polyacrylamides) a rather low glass transition for polymers **P1** (Fig. 3(b)), which approaches about 10 °C for high molar masses (Fig. 4), indicating an intramolecular plasticizer effect of the methoxyethyl groups. This value compares surprisingly well with the reported glass transition of about 5 °C for the 1:2 statistical copolymer of dimethylacrylamide **2** and 2-methoxyethylacrylate [14]. In contrast, sample **P2/HE** displayed a glass transition at about 115–120 °C, in agreement with the literature on **P2** [14, 72, 73]. Polymers **P1/HE** and **P2/HE** showed an additional small transition at about 40 °C, which is attributed to the alkyl chain terminus (Fig. 3(c)). Noteworthy, the block copolymers **P2-1a/HE** ($T_g = 80$ °C) and **P2-1b/HE** ($T_g = 58$ °C) (Fig. 3(d)) did only show one glass transition, which is located between those of the respective homopolymers and decreases with an increasing share of **P1** in the block copolymers. This suggests that the two different polyacrylamide blocks are compatible in the bulk phase.

Behavior in aqueous solution

The thermoresponsive behavior of the polymers **P1** in aqueous solution was investigated by temperature-dependent turbidimetry (see Fig. 5).

The transmission of the solutions showed a sharp transition from clear to opaque for the heating, and vice versa for the cooling runs (Fig. 5(a)). These transitions were fully reversible. The hysteresis between cooling and heating runs was very small indicating a relatively quick rehydration and resolubilization of the collapsed polymer coils. This behavior is similar to the one of PDEAm [74–76], but contrasts with the one of PNIPAm [74, 76, 77]. The different transition behaviors were attributed to the N-H group of the secondary amide

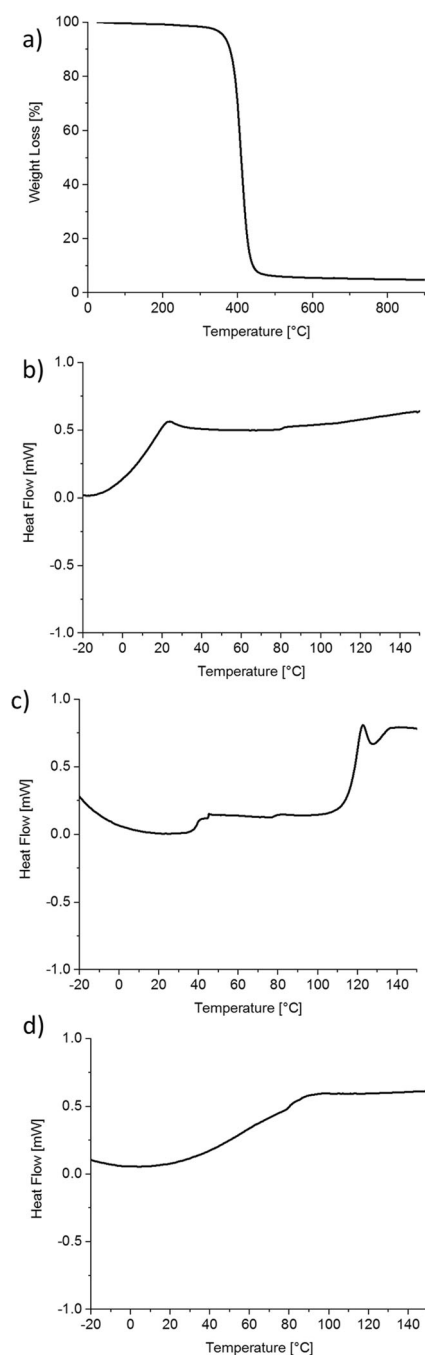


Fig. 3 Thermal analysis of homo- and copolymers of **1**: (a) TGA analysis of **P1d**, (b) DSC thermogram of **P1d**, (c) DSC thermogram of macroCTA **P2/HE**, (d) DSC thermogram of block copolymer **P2-1b/HE**

moiety specific for PNIPAm, which is assumed to enable interchain hydrogen bonds that act as “cross-linking points” inside the swollen polymer chain and delay the diffusion of water into the dense aggregates [74–77], but other kinetic effects seem also responsible [78–80]. Furthermore, the two methoxyethyl groups attached to the amide moiety of **P1** might facilitate the diffusion of water because they provide additional hydrophilicity in analogy to poly((meth)acrylate) that bear oligo (ethylene oxide) side chains [24, 46]. Up to

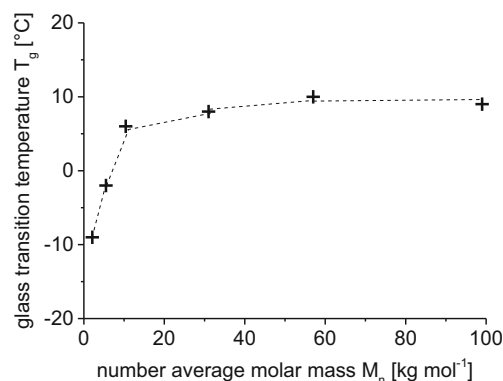


Fig. 4 Molar mass dependence of the glass transition temperatures T_g of homopolymers **P1a–f**. The broken line is meant as guide to the eye

10 g L⁻¹, the cloud points shift towards lower temperatures with increasing concentration. Except for the oligomeric sample of **P1a** with a molar mass of 1.9 kg mol⁻¹, the phase transitions of all samples slowly approached a temperature minimum with increasing concentration (Fig. 5(b)). To investigate the influence of the molar mass, homopolymers **P1a–f** were synthesized with molar masses varying from about 2 to 100 kg mol⁻¹ using CTA **3**. This CTA was chosen to introduce only rather small propyl and benzyl end groups into the polymers, in order to minimize end group effects on the LCST. Figure 5 (b) illustrates that with increasing molar mass, the cloud points are initially increasing. Only when the molar mass becomes sufficiently high at around 10 kg mol⁻¹ (**P1c**), the cloud point at 10 g L⁻¹ seems to approach a maximum temperature, reaching a plateau value of around 46 °C. This trend does not follow the classical Flory–Huggins theory, according to which polymers become less soluble with growing molar mass as the combinatorial entropy term of mixing becomes less favorable [81, 82]. We explain this behavior by the sensitivity of the coil-to-globule transition of **P1** to the presence of even small hydrophobic end groups, as known for other thermoresponsive polyacrylamides as, e.g., PNIPAm [9, 82] or poly(*N*-acryloyl pyrrolidine) PNAP [83]. With increasing length of the polymer chain, the polymer’s inherent hydrophilicity can increasingly outweigh the hydrophobic contribution of the end groups, so that the cloud point approaches an upper limiting value.

To gain a better understanding of how hydrophobic end groups influence the phase behavior of **P1**, we studied also the homopolymer **P1/HE** bearing a marked hydrophobic end group incorporating the hydrophobic dodecyl chain. Having a molar mass of around 30 kg mol⁻¹, **P1/HE** is well comparable to **P1d**, their main difference being the hydrophobicity of the end groups. For **P1/HE**, the cloud points are notably lowered to the temperature of about 42 °C compared with the cloud point of **P1d** of around 46 °C. This indicates a higher solubility for the polymer with the less hydrophobic end groups. This marked influence of the hydrophobic end group is in

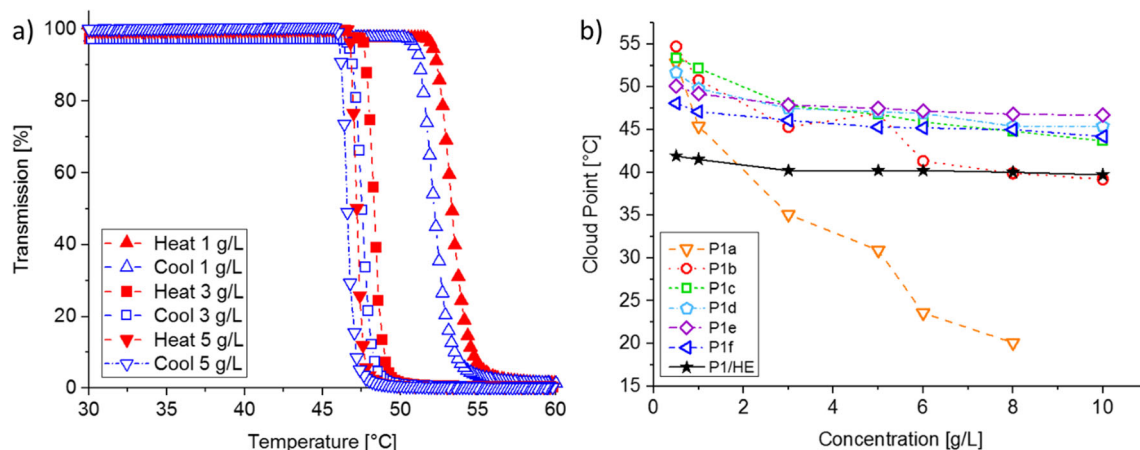


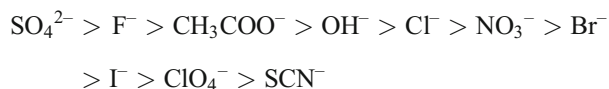
Fig. 5 Turbidimetry studies (at $\lambda = 600$ nm) of homopolymers of **1**: (a) temperature-dependent transmission for different concentrations of **P1c**, heating cycles are shown by full symbols, cooling cycles by open

symbols; (b) concentration dependence of the cloud points of homopolymers **P1** having various molar masses and/or end groups. The lines are meant as guide to the eye

agreement with the explanation proposed above for the observed increase of the cloud points with increasing molar masses up to 10 kg mol^{-1} .

We note that the limiting cloud point values of our samples approached the range between 42 and 46 °C with increasing molar masses, which is above the originally reported value of 41.5 °C by Ito [33], but lower than the values of 49.5 °C reported by Yamazaki et al. [47] and of 58.4 °C reported by Hidaka et al. [36]. These differences might be due to differing molar masses, dispersities, and/or end groups of these samples, which were synthesized by classical free radical polymerization. Also, different tacticities might be responsible taking the reports for other polyacrylamides including PDEAm into account [42, 84–86]. However, the scarce analytical data reported preclude from a more thorough discussion.

In most cases, thermoresponsive polymers are not employed in pure water, but their applications include solution additives such as salts. In addition to the effect of ionic strength, ion specific effects on the LCST have been reported, which follow the so-called Hofmeister series [87]. This series empirically describes the ability of salts to precipitate proteins from aqueous solution. This phenomenon is more pronounced for anions than for cations following the typical order:



The anions on the left side of the series are referred to as kosmotropes, originally supposed to “structure” bulk water, while those on the right side are called chaotropes originally supposed to “break” bulk water structure. Several ionic properties such as size, polarizability, hydration energetics, and the partition coefficient influence their precipitation. The presence of such anions can also influence the phase transition behavior of thermoresponsive polymers such as PNIPAm [42, 88–91]

or PDEAm [42, 92]. Consequently, we explored the effect of representative sodium salts on the cloud point of **P1** using sample **P1f** via DLS, employing the fluoride F^- that is regarded to be highly kosmotropic, the thiocyanate SCN^- that is regarded to be highly chaotropic, and the chloride Cl^- designating the dividing line between those two types (Fig. 6).

At temperatures well below the phase transition, **P1f** has a hydrodynamic diameter of ~ 25 nm which is comparable with the values reported for single PDEAM chains of similar molar mass [93]. Within the precision of the measurement, the hydrodynamic diameter seems to be unchanged upon the addition of the salts. In pure water, the cloud point of **P1f** is 45 °C. When NaCl is added, the cloud point shifts slightly towards lower temperatures. The observed rather weak salting-out effect of Cl^- was similar not only to other polyacrylamides such as PNIPAm [88, 94], PDEAm [42, 92], or PNAP [83] but also

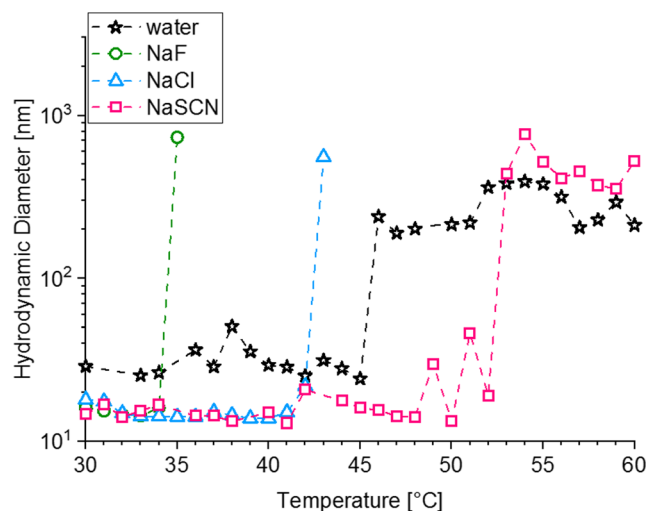


Fig. 6 Temperature-dependent hydrodynamic diameters of **P1f** in aqueous solution for different added salts from DLS (polymer concentration = 1 g L^{-1} , salt concentration = 200 mM)

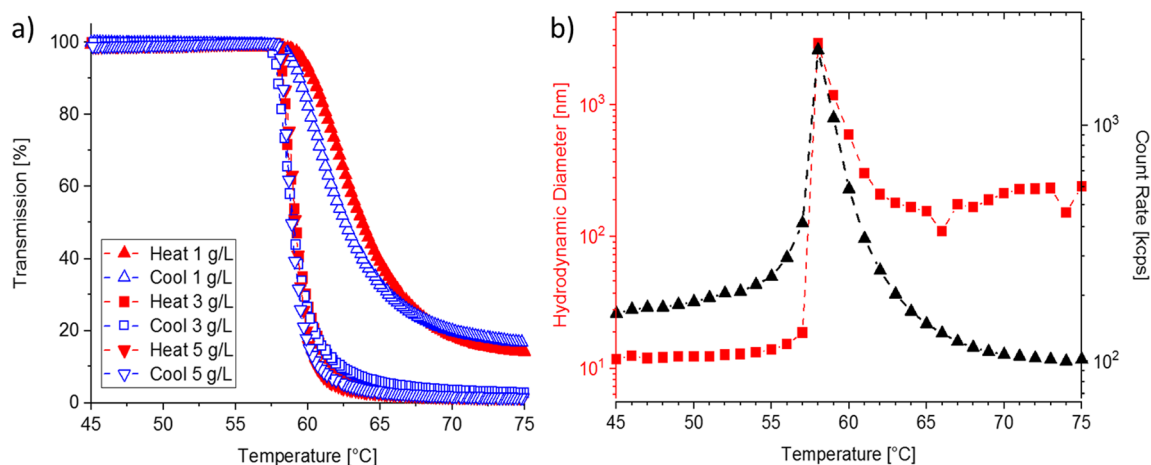


Fig. 7 Thermoresponsive behavior of **P2-1b/HE** in aqueous solution. Temperature-dependent (a) transmission for different concentrations and (b) hydrodynamic diameter for $c = 5 \text{ g L}^{-1}$. Lines are meant as a guide to the eye

to polymethacrylates bearing oligo (ethyleneglycolether) side chains [83]. The ability to lower the phase transition temperature becomes more pronounced when NaF is added. The strongly hydrated F^- induces a marked salting-out effect, decreasing the cloud point of **P1f** to 34 °C. Contrariwise, the addition of NaSCN raises the cloud point to 52 °C, clearly showing the salting-in effect of the weakly hydrated and highly polarizable SCN^- anion. The kosmotropic and chaotropic nature of F^- and SCN^- , respectively, with the corresponding salting-out and salting-in effects was also demonstrated on low dispersity PNIPAm of similar [94] and other molar masses [88, 95]. However, the influence on the phase transition temperature of PNIPAm was less pronounced than for **P1f** revealing the higher ion specific response of polymers of bMOEAm **1** to such salts.

It is interesting to note that **P1f** produced rather long-lived colloidal aggregates in pure aqueous solution above the cloud point. Such aggregates are often referred to as mesoglobules, the precise reasons for their formation still being under discussion [4, 6, 96]. Such a behavior seems typical for PNIPAm in dilute aqueous solution, for which it has been intensely studied, but has been also described occasionally for other non-ionic thermoresponsive polymers [4, 6]. Mesoglobules were reported to be destabilized when inorganic salts, typically chlorides, were added, resulting in macroscopic phase separation [6]. Figure 6 shows that this was also the case for **P1f** in the presence of NaCl or NaF, but not when adding NaSCN. On the basis of our limited experiments, it could only be speculated whether and how the sensitivity of mesoglobules to electrolytes is correlated to the kosmotropic and chaotropic nature of their anions, but this may be a point worth to be addressed in future studies for refining the understanding of the mesoglobule phenomenon.

In addition to the homopolymers, we explored the thermoresponsive behavior of the block copolymers **P2-1a/HE** and **P2-1b/HE** as potentially “smart” surfactants by DLS and turbidimetry (Fig. 7).

Both block copolymers have a hydrodynamic diameter of $\sim 10 \text{ nm}$ at temperatures well below the phase transition. This is similar to homopolymer samples **P1c-d** with comparable chain lengths as the thermoresponsive block of the copolymers has, but lower than the hydrodynamic diameter observed for the high molar mass polymers **P1e-f**. This points to a marked influence of the thermoresponsive block on the coil size in water (Fig. 7(b)), possibly due to the compatibility of the **P1** and **P2** blocks as indicated in the DSC thermograms.

Noteworthy, for **P2-1a/HE** bearing a short **P1** block with around 40 repeating units of bMOEAm, no phase transition occurred up to a concentration of 5 g L^{-1} . In contrast, when a longer thermoresponsive block of around 100 repeat units was incorporated as in **P2-1b/HE**, we observed a fully reversible phase transition with a very small hysteresis analogously to the behavior of the homopolymers. Still, the phase transition temperature increased markedly compared with the homopolymers. As demonstrated, the water solubility of polymers **P1** is strongly affected by hydrophobic end groups. Obviously, this is also the case for hydrophilic groups attached to **P1**, such as the **P2** block (PDMAM). The enhanced solubility in water increases the cloud point and shifts the phase transition to around 60 °C, which is almost 15 °C higher than for the **P1** homopolymers. Most likely, enhanced solubility accounts also for the lacking phase transition of **P2-1a/HE** in the studied temperature range, as the thermoresponsive **P1** block is apparently too short to counterbalance the effect of the strongly hydrophilic **P2** block attached. We note that structurally similar block copolymers of **P2** and PDEAm (PDMAM-b-PDEAm) showed only slightly higher phase transition temperatures compared with PDEAm homopolymers [97]. This is also the case for block copolymers of **P2** and PNIPAm [98, 99]. Accordingly, the additional ethyleneglycolether motifs in the analogous tertiary polyacrylamide **P1**, PbMOEAm, render the phase transition considerably more sensitive to attached hydrophilic blocks.

Conclusion

Homo- and block copolymers based on bMOEAm **1**, which bears both the amide and ethyleneglycolether motifs, with varying molar mass and low dispersities were synthesized by RAFT polymerization. The thermoresponsive behavior of the polymers **P1** in aqueous solution was investigated by DLS and turbidimetry as a function of the polymer concentration, molar mass, and end groups. The cloud points were found to approach a limiting value of around 46 °C with increasing concentration and molar mass. The phase transitions were fully reversible showing a very small hysteresis only, similar to PDEAm and PEG-derived vinyl polymers. The observed increase of the cloud point with increasing molar mass, which is apparently in conflict with the classical Flory–Huggins theory, is explained by the hydrophobicity of the end groups introduced by the RAFT process. Those effects are only gradually overcome with growing polymer chain length. The thermoresponsive behavior of the polymers is also influenced by the concentration of added salts and by the specific nature of their anions, following the Hofmeister series. A kosmotropic anion such as fluoride markedly decreased the cloud point, while the chaotropic thiocyanate markedly increased it. The cloud points of **P1** were stronger affected by F[−] and SCN[−] anions than reported for PNIPAm, whereas Cl[−] showed as little effect as on other polyacrylamides. Homopolymers of bMOEAm **1** bearing a strongly hydrophobic end group implemented through the CTA, as well as block copolymers containing additionally a long hydrophilic PDMAm block, were studied as potential switchable surfactants. The former design provides successfully a responsive macrosurfactant with a transition from an amphiphilic to a water-insoluble state and a transition temperature around 42 °C, i.e., in the interesting window around human body temperature. However, for the latter block copolymer design, the phase transition temperature of PbMOEAm **P1** is strongly increased when an additional hydrophilic block enhances the water solubility of the polymer. Consequently, for the block copolymer bearing a rather short block of PbMOEAm **P1**, no phase transition occurred which would convert the double hydrophilic copolymer into an amphiphilic one. Even when a rather long block of **P1** is incorporated so that a phase transition is imposed, nevertheless, the transition is shifted to an often unpractically high temperature of 60 °C. Accordingly, PbMOEAm **P1** seems not the obvious choice for constructing this type of switchable block copolymer surfactants for medical or cosmetic applications, but are interesting for applications where 'switching' is aspired at elevated temperatures. Nonetheless, double hydrophilic block copolymers containing PbMOEAm **P1** as well as the pure homopolymers represent a useful complement to established thermosensitive polymers for applications in material science and biotechnology at elevated temperatures, due to their straightforward monomer synthesis and good

polymerizability, as well as their tunable phase transition temperature.

Acknowledgments The authors gratefully acknowledge SEC support by S. Prenzel and H. Schlaad, and assistance for thermal analysis by D. Schanzenbach (Universität Potsdam). We thank Dr. Makoto Uyama (Shiseido Co.) for translating reference [33] from Japanese to English.

Funding information Open Access funding provided by Projekt DEAL. This work was supported by Deutsche Forschungsgemeinschaft (DFG), grants GR 1030/22-1 and LA 611/17-1.

Compliance with ethical standards

Conflict of interest The authors declare that they have no conflict of interest.

Open Access This article is licensed under a Creative Commons Attribution 4.0 International License, which permits use, sharing, adaptation, distribution and reproduction in any medium or format, as long as you give appropriate credit to the original author(s) and the source, provide a link to the Creative Commons licence, and indicate if changes were made. The images or other third party material in this article are included in the article's Creative Commons licence, unless indicated otherwise in a credit line to the material. If material is not included in the article's Creative Commons licence and your intended use is not permitted by statutory regulation or exceeds the permitted use, you will need to obtain permission directly from the copyright holder. To view a copy of this licence, visit <http://creativecommons.org/licenses/by/4.0/>.

References

- Cohen Stuart MA, Huck WTS, Genzer J, Müller M, Ober C, Stamm M, Sukhorukov GB, Szleifer I, Tsukruk VV, Urban M, Winnik F, Zauscher S, Luzinov I, Minko S (2010) Emerging applications of stimuli-responsive polymer materials. *Nat Mater* 9: 101–113. <https://doi.org/10.1038/nmat2614>
- Hu L, Zhang Q, Li X, Serpe MJ (2019) Stimuli-responsive polymers for sensing and actuation. *Mater Horiz* 6:1774–1793. <https://doi.org/10.1039/c9mh00490d>
- Doberenz F, Zeng K, Willems C, Zhang K, Groth T (2020) Thermoresponsive polymers and their biomedical application in tissue engineering—a review. *J Mater Chem B* 8:607–628. <https://doi.org/10.1039/c9tb02052g>
- Aseyev V, Tenhu H, Winnik F (2011) Non-ionic thermoresponsive polymers in water. *Adv Polym Sci* 242:29–89. https://doi.org/10.1007/12_2010_57
- Roy D, Brooks WLA, Sumerlin BS (2013) New directions in thermoresponsive polymers. *Chem Soc Rev* 42:7214–7243. <https://doi.org/10.1039/c3cs35499g>
- Halperin A, Kröger M, Winnik FM (2015) Poly(N-isopropylacrylamide) phase diagrams: fifty years of research. *Angew Chem Int Ed* 54:15342–15367. <https://doi.org/10.1002/anie.201506663>
- Lutz J-F (2008) Polymerization of oligo (ethylene glycol) (meth)acrylates: toward a new generation of smart biocompatible materials. *J Polym Sci Part A Polym Chem* 46:3459–3470
- Badi N (2017) Non-linear PEG-based thermoresponsive polymer systems. *Prog Polym Sci* 66:54–79. <https://doi.org/10.1016/j.progpolymsci.2016.12.006>

9. Furyk S, Zhang Y, Ortiz-Acosta D, Cremer PS, Bergbreiter DE (2006) Effects of end group polarity and molecular weight on the lower critical solution temperature of poly(N-isopropylacrylamide). *J Polym Sci Part A Polym Chem* 44:1492–1501. <https://doi.org/10.1002/pola.21256>
10. Roth PJ, Jochum FD, Forst FR, Zentel R, Theato P (2010) Influence of end groups on the stimulus-responsive behavior of poly [oligo (ethylene glycol) methacrylate] in water. *Macromolecules* 43:4638–4645. <https://doi.org/10.1021/ma1005759>
11. Xia Y, Burke NAD, Stöver HDH (2006) End group effect on the thermal response of narrow-disperse poly(N-isopropylacrylamide) prepared by atom transfer radical polymerization. *Macromolecules* 39:2275–2283
12. Nord FF, Bier M, Timasheff SN (1951) Investigations on proteins and polymers. IV Critical phenomena in polyvinyl alcohol-acetate copolymer solutions. *J Am Chem Soc* 73:289–293
13. Mueller KF (1992) Thermotropic aqueous gels and solutions of N, N-dimethylacrylamide-acrylate copolymers. *Polymer* 33:3470–3476. [https://doi.org/10.1016/0032-3861\(92\)91105-B](https://doi.org/10.1016/0032-3861(92)91105-B)
14. El-Ejmi AAS, Huglin MB (1996) Characterization of N,N-dimethylacrylamide/2-methoxyethylacrylate copolymers and phase behaviour of their thermotropic aqueous solutions. *Polym Int* 39:113–119. [https://doi.org/10.1002/\(sici\)1097-0126\(199602\)39:2<113::Aid-pi476>3.0.Co;2-c](https://doi.org/10.1002/(sici)1097-0126(199602)39:2<113::Aid-pi476>3.0.Co;2-c)
15. Chytrý V, Netopilík M, Bohdanecký M, Ulbrich K (1997) Phase transition parameters of potential thermosensitive drug release systems based on polymers of N-alkylmethacrylamides. *J Biomater Sci Polym Ed* 8:817–824. <https://doi.org/10.1163/156856297x00010>
16. Liu R, Fraylich M, Saunders BR (2009) Thermoresponsive copolymers: from fundamental studies to applications. *Colloid Polym Sci* 287:627–643. <https://doi.org/10.1007/s00396-009-2028-x>
17. Kokufuta MK, Sato S, Kokufuta E (2012) LCST behavior of copolymers of N-isopropylacrylamide and N-isopropylmethacrylamide in water. *Colloid Polym Sci* 290:1671–1681. <https://doi.org/10.1007/s00396-012-2706-y>
18. Ritter H, Stock A (1994) Synthesis of thermoreversible polymers by aminolysis of poly (methyl 2-(N-acryloylamino)-2-methoxyacetate): correlations of the lower critical solution temperatures (LCST) with the side group structures and the salt concentration in aqueous systems. *Macromol Rapid Commun* 15:271–277. <https://doi.org/10.1002/marc.1994.030150314>
19. Laschewsky A, Rekaí ED, Wischerhoff E (2001) Tailoring of stimuli-responsive water-soluble acrylamide and methacrylamide polymers. *Macromol Chem Phys* 202:276–286. [https://doi.org/10.1002/1521-3935\(20010101\)202:2<276::AID-MACP276>3.0.CO;2-1](https://doi.org/10.1002/1521-3935(20010101)202:2<276::AID-MACP276>3.0.CO;2-1)
20. Jochum FD, Theato P (2009) Temperature- and light-responsive polyacrylamides prepared by a double polymer analogous reaction of activated ester polymers. *Macromolecules* 42:5941–5945. <https://doi.org/10.1021/ma900945s>
21. Zhu Y, Batchelor R, Lowe AB, Roth PJ (2016) Design of thermoresponsive polymers with aqueous LCST, UCST, or both: modification of a reactive poly(2-vinyl-4,4-dimethylazlactone) scaffold. *Macromolecules* 49:672–680. <https://doi.org/10.1021/acs.macromol.5b02056>
22. Priest JH, Murray SL, Nelson RJ, Hoffman AS (1987) Lower critical solution temperatures of aqueous copolymers of N-isopropylacrylamide and other N-substituted acrylamides. *ACS Symp Ser* 350:255–264
23. Liu HY, Zhu XX (1999) Lower critical solution temperatures of N-substituted acrylamide copolymers in aqueous solutions. *Polymer* 40:6985–6990. [https://doi.org/10.1016/S0032-3861\(98\)00858-1](https://doi.org/10.1016/S0032-3861(98)00858-1)
24. Lutz J-F, Akdemir Ö, Hoth A (2006) Point by point comparison of two thermosensitive polymers exhibiting a similar LCST: is the age of poly (NIPAM) Over? *J Am Chem Soc* 128:13046–13047
25. Keerl M, Richtering W (2007) Synergistic depression of volume phase transition temperature in copolymer microgels. *Colloid Polym Sci* 285:471–474
26. Weiss J, Li A, Wischerhoff E, Laschewsky A (2012) Water-soluble random and alternating copolymers of styrene monomers with adjustable lower critical solution temperature. *Polym Chem* 3:352–361. <https://doi.org/10.1039/c1py00422k>
27. Kermagoret A, Fustin C-A, Bourguignon M, Detrembleur C, Jerome C, Debuigne A (2013) One-pot controlled synthesis of double thermoresponsive N-vinylcaprolactam-based copolymers with tunable LCSTs. *Polym Chem* 4:2575–2583. <https://doi.org/10.1039/c3py00134b>
28. Buller J, Laschewsky A, Lutz J-F, Wischerhoff E (2011) Tuning the lower critical solution temperature of thermoresponsive polymers by biospecific recognition. *Polym Chem* 2:1486–1489. <https://doi.org/10.1039/c1py00001b>
29. Couturier J-P, Sütterlin M, Laschewsky A, Hettrich C, Wischerhoff E (2015) Responsive inverse opal hydrogels for the sensing of macromolecules. *Angew Chem Int Ed* 54:6641–6644. <https://doi.org/10.1002/anie.201500674>
30. Eggers S, Eckert T, Abetz V (2018) Double thermoresponsive block–random copolymers with adjustable phase transition temperatures: from block-like to gradient-like behavior. *J Polym Sci Part A Polym Chem* 56:399–411. <https://doi.org/10.1002/pola.28906>
31. Kudo Y, Mori H, Kotsuchibashi Y (2018) Preparation of an ethylene glycol-based block copolymer consisting of six different temperature-responsive blocks. *Polym J (Jpn)* 50:1013–1020. <https://doi.org/10.1038/s41428-018-0091-1>
32. Yamano T, Higashi N, Koga T (2020) Precisely synthesized sequence-controlled amino acid-derived vinyl polymers: new insights into thermo-responsive polymer design. *Macromol Rapid Commun* 41(1900550):1900551–1900558. <https://doi.org/10.1002/marc.201900550>
33. Ito S (1990) Phase transition of aqueous solutions of poly(N-alkoxyalkylacrylamide) derivatives. Effects of side chain structure. *Kobunshi Ronbunshu* 47:467–474. <https://doi.org/10.1295/koron.47.467>
34. Terada T, Inaba T, Kitano H, Maeda Y, Tsukida N (1994) Raman spectroscopic study on water in aqueous solutions of temperature-responsive polymers: poly(N-isopropylacrylamide) and poly [N-(3-ethoxypropyl)acrylamide]. *Makromol Chem* 195:3261–3270. <https://doi.org/10.1002/macp.1994.021950922>
35. Chua GBH, Roth PJ, Duong HTT, Davis TP, Lowe AB (2012) Synthesis and thermoresponsive solution properties of poly [oligo (ethylene glycol) (meth)acrylamide]: biocompatible PEG analogues. *Macromolecules* 45:1362–1374. <https://doi.org/10.1021/ma202700y>
36. Hidaka T, Sugihara S, Maeda Y (2013) Infrared spectroscopic study on LCST behavior of poly(N,N-bis(2-methoxyethyl)acrylamide). *Eur Polym J* 49:675–681. <https://doi.org/10.1016/j.eurpolymj.2013.01.002>
37. Kawatani R, Kawata Y, S-i Y, Kelland MA, Ajiro H (2018) Synthesis of thermosensitive poly(N-vinylamide) derivatives bearing oligo ethylene glycol chain for kinetic hydrate inhibitor. *Macromolecules* 51:7845–7852. <https://doi.org/10.1021/acs.macromol.8b01573>
38. Sedlacek O, Bera D, Hoogenboom R (2019) Poly(2-amino-2-oxazoline)s: a new class of thermoresponsive polymers. *Polym Chem* 10:4683–4689. <https://doi.org/10.1039/C9PY00943D>
39. Quek JY, Zhu Y, Roth PJ, Davis TP, Lowe AB (2013) RAFT Synthesis and aqueous solution behavior of novel pH- and thermo-responsive (co) polymers derived from reactive poly(2-vinyl-4,4-dimethylazlactone) scaffolds. *Macromolecules* 46:7290–7302. <https://doi.org/10.1021/ma4013187>
40. Trzebicka B, Szweida D, Rangelov S, Kowalczyk A, Mendrek B, Utrata-Wesołek A, Dworak A (2013) (Co) polymers of oligo

- (ethylene glycol) methacrylates—temperature-induced aggregation in aqueous solution. *J Polym Sci Part A Polym Chem* 51:614–623. <https://doi.org/10.1002/pola.26410>
41. Vancouillie G, Frank D, Hoogenboom R (2014) Thermoresponsive poly (oligo ethylene glycol acrylates). *Progr Polym Sci* 39:1074–1095. <https://doi.org/10.1016/j.progpolymsci.2014.02.005>
 42. Baltes T, Garret-Flaudy F, Freitag R (1999) Investigation of the LCST of polyacrylamides as a function of molecular parameters and the solvent composition. *J Polym Sci Part A Polym Chem* 37: 2977–2989. [https://doi.org/10.1002/\(SICI\)1099-0518\(19990801\)37:15<2977::AID-POLA31>3.0.CO;2-I](https://doi.org/10.1002/(SICI)1099-0518(19990801)37:15<2977::AID-POLA31>3.0.CO;2-I)
 43. Plamper FA, Steinschulte AA, Hofmann CH, Drude N, Mergel O, Herbert C, Erberich M, Schulte B, Winter R, Richtering W (2012) Toward copolymers with ideal thermosensitivity: solution properties of linear, well-defined polymers of N-isopropyl acrylamide and N,N-diethyl acrylamide. *Macromolecules* 45:8021–8026. <https://doi.org/10.1021/ma301606c>
 44. Watanabe R, Takaseki K, Katsumata M, Matsushita D, Ida D, Osa M (2016) Characterization of poly(N,N-diethylacrylamide) and cloud points in its aqueous solutions. *Polym J (Jpn)* 48:621–628. <https://doi.org/10.1038/pj.2015.120>
 45. Hua F, Jiang X, Li D, Zhao B (2006) Well-defined thermosensitive, water-soluble polyacrylates and polystyrenics with short pendant oligo (ethylene glycol) groups synthesized by nitroxide-mediated radical polymerization. *J Polym Sci Part A Polym Chem* 44:2454–2467
 46. Miasnikova A, Laschewsky A (2012) Influencing the phase transition temperature of poly (methoxy diethylene glycol acrylate) by molar mass, end groups, and polymer architecture. *J Polym Sci Part A Polym Chem* 50:3313–3323. <https://doi.org/10.1002/pola.26116>
 47. Yamazaki A, Song JM, Winnik FM, Brash JL (1998) Synthesis and solution properties of fluorescently labeled amphiphilic (N-alkylacrylamide) oligomers. *Macromolecules* 31:109–115. <https://doi.org/10.1021/ma971111u>
 48. Yamazaki A, Winnik FM, Cornelius RM, Brash JL (1999) Modification of liposomes with N-substituted polyacrylamides: identification of proteins adsorbed from plasma. *Biochim Biophys Acta Biomembr* 1421:103–115. [https://doi.org/10.1016/S0005-2736\(99\)00117-0](https://doi.org/10.1016/S0005-2736(99)00117-0)
 49. El-Ejmi AAS, Huglin MB (1997) Behaviour of poly(N,N-dimethylacrylamide-co-2-methoxyethylacrylate) in non-aqueous solution and LCST behaviour in water. *Eur Polym J* 33:1281–1284. [https://doi.org/10.1016/S0014-3057\(96\)00272-8](https://doi.org/10.1016/S0014-3057(96)00272-8)
 50. Haraguchi K, Kubota K, Takada T, Mahara S (2014) Highly protein-resistant coatings and suspension cell culture thereon from amphiphilic block copolymers prepared by RAFT polymerization. *Biomacromolecules* 15:1992–2003. <https://doi.org/10.1021/bm401914c>
 51. Bivigou-Koumba AM, Kristen J, Laschewsky A, Müller-Buschbaum P, Papadakis CM (2009) Synthesis of symmetrical triblock copolymers of styrene and N-isopropylacrylamide using bifunctional bis (trithiocarbonate) s as RAFT agents. *Macromol Chem Phys* 210:565–578. <https://doi.org/10.1002/macp.200800575>
 52. Schweizerhof S, Demco DE, Mourran A, Keul H, Fehete R, Möller M (2017) Temperature-induced phase transition characterization of responsive polymer brushes grafted onto nanoparticles. *Macromol Chem Phys* 218(1600495):1600491–1600411. <https://doi.org/10.1002/macp.201600495>
 53. Zhao Y, Perrier S (2007) Reversible addition-fragmentation chain transfer graft polymerization mediated by fumed silica supported chain transfer agents. *Macromolecules* 40:9116–9124. <https://doi.org/10.1021/ma0716783>
 54. Roth M, Oesterreicher A, Mostegel FH, Moser A, Pinter G, Edler M, Piock R, Griesser T (2016) Silicon-based mercaptans: high-performance monomers for thiol-ene photopolymerization. *J Polym Sci Part A Polym Chem* 54:418–424. <https://doi.org/10.1002/pola.27792>
 55. Skrabania K, Miasnikova A, Bivigou-Koumba AM, Zehm D, Laschewsky A (2011) Examining the UV-vis absorption of RAFT chain transfer agents, and their use for polymer analysis. *Polym Chem* 2:2074–2083. <https://doi.org/10.1039/c1py00173f>
 56. Flynn JH (1974) Thermodynamic properties from differential scanning calorimetry by calorimetric methods. *Thermochim Acta* 8:69–81. [https://doi.org/10.1016/0040-6031\(74\)85073-2](https://doi.org/10.1016/0040-6031(74)85073-2)
 57. Moad G, Rizzardo E, Thang SH (2008) Toward living radical polymerization. *Acc Chem Res* 41:1133–1142. <https://doi.org/10.1021/ar800075n>
 58. Lai JT, Filla D, Shea R (2002) Functional polymers from novel carboxyl-terminated trithiocarbonates as highly efficient RAFT agents. *Macromolecules* 35:6754–6756. <https://doi.org/10.1021/ma020362m>
 59. Ganeva DE, Sprong E, Hd B, Warr GG, Such CH, Hawkett BS (2007) Particle formation in ab initio RAFT mediated emulsion polymerization systems. *Macromolecules* 40:6181–6189
 60. Samakande A, Chaghi R, Derrien G, Charnay C, Hartmann PC (2008) Aqueous behaviour of cationic surfactants containing a cleavable group. *J Colloid Interface Sci* 320:315–320. <https://doi.org/10.1016/j.jcis.2008.01.022>
 61. Rieger J, Osterwinter G, Bui C, Stoffelbach F, Charleux B (2009) Surfactant-free controlled/living radical emulsion (Co) polymerization of n-butyl acrylate and methyl methacrylate via RAFT using amphiphilic poly (ethylene oxide)-based trithiocarbonate chain transfer agents. *Macromolecules* 42:5518–5525. <https://doi.org/10.1021/ma9008803>
 62. Herfurth C, Malo de Molina P, Wieland C, Rogers SH, Gradzielski M, Laschewsky A (2012) One-step RAFT synthesis of well-defined amphiphilic star polymers and their self-assembly in aqueous solution. *Polym Chem* 3:1606–1617. <https://doi.org/10.1039/c2py20126g>
 63. Ren H, Qiu X-P, Shi Y, Yang P, Winnik FM (2019) pH-dependent morphology and photoresponse of azopyridine-terminated poly(N-isopropylacrylamide) nanoparticles in water. *Macromolecules* 52: 2939–2948. <https://doi.org/10.1021/acs.macromol.9b00193>
 64. Ohnsorg ML, Ting JM, Jones SD, Jung S, Bates FS, Reineke TM (2019) Tuning PNIPAm self-assembly and thermoresponse: roles of hydrophobic end-groups and hydrophilic comonomer. *Polym Chem* 10:3469–3479. <https://doi.org/10.1039/C9PY00180H>
 65. Päch M, Zehm D, Lange M, Dambowsky I, Weiss J, Laschewsky A (2010) Universal polymer analysis by ¹H NMR using complementary trimethylsilyl end groups. *J Am Chem Soc* 132:8757–8765. <https://doi.org/10.1021/ja102096u>
 66. Weiss J, Laschewsky A (2011) Temperature induced self-assembly of triple responsive triblock copolymers in aqueous solutions. *Langmuir* 27:4465–4473. <https://doi.org/10.1021/la200115p>
 67. Marsat J-N, Heydenreich M, Kleinpeter E, Laschewsky A, von Berlepsch H, Böttcher C (2011) Self-assembly into multicompartement micelles, and selective solubilization by hydrophilic-lipophilic-fluorophilic block copolymers. *Macromolecules* 44:2092–2105. <https://doi.org/10.1021/ma200032j>
 68. Fischer F, Zufferey D, Tahoces R (2011) Lower critical solution temperature in superheated water: the highest in the poly(N,N-dialkylacrylamide) series. *Polym Int* 60:1259–1262. <https://doi.org/10.1002/pi.3071>
 69. Laschewsky A, Herfurth C, Miasnikova A, Stahlhut F, Weiss J, Wieland C, Wischerhoff E, Gradzielski M, Malo de Molina P (2013) Stars and blocks: tailoring polymeric rheology modifiers for aqueous media by controlled free radical polymerization. *ACS Symp Ser* 1148:125–143. <https://doi.org/10.1021/bk-2009-1023.ch013>

70. Moad G, Chong YK, Postma A, Rizzardo E, Thang SH (2005) Advances in RAFT polymerization: the synthesis of polymers with defined end-groups. *Polymer* 46:8458–8468. <https://doi.org/10.1016/j.polymer.2004.12.061>
71. Laschewsky A, Pound G, Skrabania K, Holdt HJ, Teller J (2007) Unsymmetrical bifunctional trithiocarbonate as unexpected by-product in the synthesis of a dithioester RAFT-agent. *Colloid Polym Sci* 285:947–952. <https://doi.org/10.1007/s00396-007-1653-5>
72. Köberle P, Laschewsky A, van den Boogaard D (1992) Self-organization of hydrophobized polyzwitterions. *Polymer* 33:4029–4039. [https://doi.org/10.1016/0032-3861\(92\)90601-r](https://doi.org/10.1016/0032-3861(92)90601-r)
73. Bennour S, Louzri F (2014) Study of swelling properties and thermal behavior of poly(N,N-dimethylacrylamide-co-maleic acid) based hydrogels. *Adv Chem* 147398:147391–147310. <https://doi.org/10.1155/2104/147398>
74. Zhou K, Lu Y, Li J, Shen L, Zhang G, Xie Z, Wu C (2008) The coil-to-globule-to-coil transition of linear polymer chains in dilute aqueous solutions: effect of intrachain hydrogen bonding. *Macromolecules* 41:8927–8931. <https://doi.org/10.1021/ma8019128>
75. Lu Y, Zhou K, Ding Y, Zhang G, Wu C (2010) Origin of hysteresis observed in association and dissociation of polymer chains in water. *Phys Chem Chem Phys* 12:3188–3194. <https://doi.org/10.1039/b918969f>
76. Pühse M, Keerl M, Scherzinger C, Richtering W, Winter R (2010) Influence of pressure on the state of poly(N-isopropylacrylamide) and poly(N,N-diethylacrylamide) derived polymers in aqueous solution as probed by FTIR-spectroscopy. *Polymer* 51:3653–3659. <https://doi.org/10.1016/j.polymer.2010.06.011>
77. Cheng H, Shen L, Wu C (2006) LLS and FTIR studies on the hysteresis in association and dissociation of poly(N-isopropylacrylamide) chains in water. *Macromolecules* 39:2325–2329. <https://doi.org/10.1021/ma052561m>
78. Meier-Koll A, Pipich V, Busch P, Papadakis CM, Müller-Buschbaum P (2012) Phase separation in semidilute aqueous poly(N-isopropylacrylamide) solutions. *Langmuir* 28:8791–8798. <https://doi.org/10.1021/la301533z>
79. Philipp M, Kyriakos K, Silvi L, Lohstroh W, Petry W, Krüger JK, Papadakis CM, Müller-Buschbaum P (2014) From molecular dehydration to excess volumes of phase-separating PNIPAM solutions. *J Phys Chem B* 118:4253–4260. <https://doi.org/10.1021/jp501539z>
80. Futscher MH, Philipp M, Müller-Buschbaum P, Schulte A (2017) The role of backbone hydration of poly(N-isopropyl acrylamide) across the volume phase transition compared to its monomer. *Sci Rep* 7(17012):17011–17010. <https://doi.org/10.1038/s41598-017-17272-7>
81. Dormidontova EE (2002) Role of competitive PEO–water and water–water hydrogen bonding in aqueous solution PEO behavior. *Macromolecules* 35:987–1001. <https://doi.org/10.1021/ma010804e>
82. Xia Y, Yin X, Burke NAD, Stöver HDH (2005) Thermal response of narrow-disperse poly(N-isopropylacrylamide) prepared by atom transfer radical polymerization. *Macromolecules* 38:5937–5943. <https://doi.org/10.1021/ma050261z>
83. Skrabania K, Kristen J, Laschewsky A, Akdemir Ö, Hoth A, Lutz J-F (2007) Design, synthesis, and aqueous aggregation behavior of nonionic single and multiple thermoresponsive polymers. *Langmuir* 23:84–93. <https://doi.org/10.1021/la061509w>
84. Katsumoto Y, Etoh Y, Shimoda N (2010) Phase diagrams of stereocontrolled poly(N,N-diethylacrylamide) in water. *Macromolecules* 43:3120–3121. <https://doi.org/10.1021/ma902673z>
85. Munk T, Baldursdottir S, Hietala S, Rades T, Nuopponen M, Kalliomäki K, Tenhu H, Rantanen J, Strachan CJ (2013) Investigation of the phase separation of PNIPAM using infrared spectroscopy together with multivariate data analysis. *Polymer* 54:6947–6953. <https://doi.org/10.1016/j.polymer.2013.10.033>
86. Biswas CS, Hazer B (2015) Synthesis and characterization of stereoregular poly(N-ethylacrylamide) hydrogel by using Y (OTf)₃ Lewis acid. *Colloid Polym Sci* 293:143–152. <https://doi.org/10.1007/s00396-014-3399-1>
87. Salis A, Ninham BW (2014) Models and mechanisms of Hofmeister effects in electrolyte solutions, and colloid and protein systems revisited. *Chem Soc Rev* 43:7358–7377. <https://doi.org/10.1039/c4cs00144c>
88. Zhang Y, Furryk S, Bergbreiter DE, Cremer PS (2005) Specific ion effects on the water solubility of macromolecules: PNIPAM and the Hofmeister series. *J Am Chem Soc* 127:14505–14510. <https://doi.org/10.1021/ja0546424>
89. Du H, Wickramasinghe R, Qian X (2010) Effects of salt on the lower critical solution temperature of poly(N-Isopropylacrylamide). *J Phys Chem B* 114:16594–16604. <https://doi.org/10.1021/jp105652c>
90. Maeda Y, Nakamura T, Ikeda I (2001) Changes in the hydration states of poly(N-alkylacrylamide) s during their phase transitions in water observed by FTIR spectroscopy. *Macromolecules* 34:1391–1399. <https://doi.org/10.1021/ma001306t>
91. Bruce EE, Bui PT, Rogers BA, Cremer PS, van der Vegt NFA (2019) Nonadditive ion effects drive both collapse and swelling of thermoresponsive polymers in water. *J Am Chem Soc* 141:6609–6616. <https://doi.org/10.1021/jacs.9b00295>
92. Idziak I, Avoce D, Lessard D, Gravel D, Zhu XX (1999) Thermosensitivity of aqueous solutions of poly(N,N-diethylacrylamide). *Macromolecules* 32:1260–1263. <https://doi.org/10.1021/ma981171f>
93. Lessard DG, Ousalem M, Zhu XX, Eisenberg A, Carreau PJ (2003) Study of the phase transition of poly(N,N-diethylacrylamide) in water by rheology and dynamic light scattering. *J Polym Sci B Polym Phys* 41:1627–1637. <https://doi.org/10.1002/polb.10517>
94. Suwa K, Yamamoto K, Akashi M, Takano K, Tanaka N, Kunugi S (1998) Effects of salt on the temperature- and pressure-responsive properties of poly(N-vinylisobutyramide) aqueous solutions. *Colloid Polym Sci* 276:529–533. <https://doi.org/10.1007/s003960050276>
95. Zajforoushan Moghaddam S, Thormann E (2017) Hofmeister effect on PNIPAM in bulk and at an interface: surface partitioning of weakly hydrated anions. *Langmuir* 33:4806–4815. <https://doi.org/10.1021/acs.langmuir.7b00953>
96. Niebuur B-J, Chiappisi L, Jung F, Zhang X, Schulte A, Papadakis CM (2019) Kinetics of mesoglobule formation and growth in aqueous poly(N-isopropylacrylamide) solutions: pressure jumps at low and at high pressure. *Macromolecules* 52:6416–6427. <https://doi.org/10.1021/acs.macromol.9b00937>
97. Herfurth C, Laschewsky A, Noirez L, von Lospichl B, Gradzielski M (2016) Thermoresponsive (star) block copolymers from one-pot sequential RAFT polymerizations and their self-assembly in aqueous solution. *Polymer* 107:422–433. <https://doi.org/10.1016/j.polymer.2016.09.089>
98. Convertine AJ, Lokitz BS, Vasileva Y, Myrick LJ, Scales CW, Lowe AB, McCormick CL (2006) Direct synthesis of thermally responsive DMA/NIPAM diblock and DMA/NIPAM/DMA triblock copolymers via aqueous, room temperature RAFT polymerization. *Macromolecules* 39:1724–1730. <https://doi.org/10.1021/ma0523419>
99. Skrabania K, Li W, Laschewsky A (2008) Synthesis of double-hydrophilic BAB triblock copolymers via RAFT polymerisation and their thermoresponsive self-assembly in water. *Macromol Chem Phys* 209:1389–1403. <https://doi.org/10.1002/macp.200800108>